Journal of Statistical Physics, Vol. 86, Nos. 1/2, 1997

Hausdorff Dimension of Regular Points in Stochastic Burgers Flows with Lévy α-Stable Initial Data

A. W. Janicki[1] and W. A. Woyczynski[2]

Received February 22, 1995; final February 9, 1996

This paper studies statistical properties of shocks for the inviscid Burgers equation with an α-stable Lévy motion initial data. In the absence of analytic results, numerical and computer simulation tools are utilized. Qualitative and quantitative information on the scaling properties of Lagrangian regular points of solutions is obtained and, in particular, their Hausdorff dimension is estimated to be $1/\alpha$. This suggests a possible extension of Ya. Sinai's result for Brownian initial data.

KEY WORDS: Burgers equation; shocks; Hausdorff dimension; α-stable process.

1. INTRODUCTION

The Burgers equation

$$\partial_t u + u\,\partial_x u = \nu\,\partial_{xx} u, \qquad \nu = \text{const} > 0 \tag{1.1}$$

where $u = u(t, x)$ for $t > 0$, $x \in \mathbb{R}$, and $u(0, x) = u_0(x)$, is essentially a simplified version of the Navier–Stokes equation with the pressure term and the incompressibility condition omitted. It has been widely used in the physical literature as a model equation for a variety of phenomena, such as shock waves in hydrodynamic turbulence (when $\nu \searrow 0$), gas dynamics and evolution of self-gravitating sticky matter in large spatiotemporal scales of the universe (see, e.g., refs. 4, 9, 23, and 31). The equation also arises as a conservation law in the following generic situation: consider a flow of $u(t, x)$ (say, describing the density per unit length of a certain quantity) on

[1] Institute of Mathematics, Technical University, Wrocław, Poland.
[2] Department of Statistics and Center for Stochastic and Chaotic Processes in Science and Technology, Case Western Reserve University, Cleveland, Ohio 44106.

0022-4715/97/0100-0277$12.50/0

the real line with the flux of this quantity through section at x described by another function $\phi = \phi(t, x)$. Assume that the flow is subject to a conservation law

$$\frac{\partial}{\partial t}\int_{x_0}^{x_1} u(t, x)\, dx + \phi(t, x_1) - \phi(t, x_0) = 0$$

when $x_0 < x_1$. If we assume that the flux $\phi(t, x) = \Phi(u(t, x))$ depends on the local density only, then, as $x_0 \to x_1$, the above conservation law leads to an equation of Riemann type

$$\partial_t u - \Phi'(u)\, \partial_x u = 0$$

If the flux function is permitted to depend additionally on the gradient of the density u as $\phi(t, x) = \Phi(u(t, x)) - \nu\, \partial_x u(t, x)$, then the above conservation law leads to the equation

$$\partial_t u - \Phi'(u)\, \partial_x u = \nu\, \partial_{xx} u$$

of which the Burgers equation is a special case.

The Hopf–Cole substitution $\psi(t, x; \nu) = 2\nu \ln \theta(t, x)$, involving the velocity potential function $\psi = \psi(t, x) = \psi(t, x; \nu)$ defined by the relation $u = -\partial_x \psi$, transforms the nonlinear Burgers equation into the linear diffusion equation for $\theta = \theta(t, x)$, thereby leading to the explicit formula for the velocity potential

$$\psi(t, x; \nu) = 2\nu \ln \left\{ (4\pi\nu t)^{-1/2} \int_{-\infty}^{\infty} \exp\left[\frac{1}{2\nu} \left(\psi_0(a) - \frac{(x-a)^2}{2t} \right) \right] da \right\} \quad (1.2)$$

where $\psi_0 = \psi_0(a)$ is the initial velocity potential ($u_0 = -\partial_x \psi_0$).

The velocity function $u = u(t, x) = u(t, x; \nu)$ can then be expressed explicitly in the following way:

$$u(t, x; \nu) = t^{-1} \frac{Z(t, x; \nu)}{I(t, x; \nu)} \quad (1.3)$$

where

$$Z(t, x; \nu) = \int_{\mathbb{R}} (x - y) \exp\left(\frac{\psi_0(y)}{2\nu} - \frac{(x-y)^2}{4\nu t} \right) dy$$

$$I(t, x; \nu) = \int_{\mathbb{R}} \exp\left(\frac{\psi_0(y)}{2\nu} - \frac{(x-y)^2}{4\nu t} \right) dy$$

In the present paper we discuss the Burgers equation model with random initial data, in which case its solutions are also referred to as Burgers turbulence [see ref. 30 and 31 for recent surveys].

At the mathematical level, several recent papers (see, e.g., refs. 1, 3, 7, 11, 21, and 26–28) have discussed the asymptotic behavior of the rescaled random field $u(t, x; \nu)$ as $t \to \infty$ or as $\nu \to 0$, assuming that the initial data $u_0(x)$ are various stochastic processes (or random fields if the 3D analog of the above Burgers equation was being considered).

In particular, Rosenblatt[21] assumes that u_0 is an asymptotically uncorrelated stationary process and shows that, under some additional technical conditions, a centered and rescaled velocity potential $\int u(t, x; \nu)\, dx$ converges weakly to the Brownian motion process. Bulinski and Molchanov[3] and Albeverio *et al.*[1] deal with Gaussian scaling limits for initial shot noise and stationary fields with regular spectral density data, where $u(t, x; \nu)$ obeys a "Gaussian scenario" of the central limit theorem type. Surgailis *et al.*[7, 26–28] obtain a classification of (not necessarily Gaussian) scaling limits for a variety of initial processes and random fields, which include Gaussian stationary fields with singular spectral densities and shot noise processes driven by Cox–Gibbs processes, i.e., doubly stochastic Poisson processes with random intensity, which takes into account a potential of interaction between different "bumps."

If the initial fluctuations $\psi_0(x)$ are large enough to make the exponential moments of $\psi_0(x)$ infinite, and the marginal tail distribution function

$$\mathbf{P}[\exp(\psi_0(x)/(2\nu)) > y]$$

varies slowly as $y \to \infty$, then the behavior of $u(t, x)$ is very different from the "Gaussian scenario," namely

$$u(t, x) \sim \frac{x - a(t, x)}{t} \qquad (t \to \infty) \tag{1.4}$$

where $a = a(t, x)$ is the point maximizing the right-hand side of (2.1) below. For a degenerate shot noise process $\psi_0(x)$, the asymptotics (1.4), together with an estimate of growth of the right-hand side of (1.4), was rigorously established in ref. 1.

In their important physical work, Gurbatov *et al.*[9] discussed the asymptotics of $u(t, x)$ at high Reynolds numbers, in the case when the initial Gaussian data $\psi_0(x)$ are characterized by large "amplitude" $\sigma = [\mathbf{E}(\psi_0(0))^2]^{1/2}$ and large "internal scale" $L = \sigma/\sigma^* \gg 1$, where $\sigma^* = [\mathbf{E}(\psi^*(0))^2]^{1/2}$. At time $t = t_L \sim l_L(t_L)$, where

$$l_L(t) = (\sigma t)^{1/2} [\log(\sigma' t/2\pi L)]^{-1/4}$$

is the "external scale" at time t, they demonstrated (at the physical level of rigor) that "... a strongly nonlinear regime of sawtooth waves ... is set up, ... and the field's statistical properties become self-preserving" (ref. 9, p. 163). In particular, they were able to find explicitly one- and two-point distribution functions of the (limit) sawtooth velocity process (ref. 9, Section 5.4). Those ideas have been proven rigorously in ref. 20.

A recent analysis, from the viewpoint of fluid mechanics, of statistics of decaying Burgers turbulence can be found in ref. 8.

Kida[17] was one of the first to attempt to characterize the distribution of shock strengths. His result can be equivalently formulated with the use of scaling relations in the following way:

$$N(s) \propto t^{1/6} s^{1/2} \qquad \text{for} \quad s \ll 1 \tag{1.5}$$

where $N(s)$ represents the number of shocks per unit length in a single realization of $u(t, x)$, having strength of order s. Hu and Woyczynski[12] calculated the shock density in Burgers turbulence based on asymptotic results of Albeverio *et al.*[1] and Molchanov *et al.*[20]

She *et al.*[24] simulated the sawtooth profiles appearing in the solution to the inviscid Burgers equation with self-similar random data (with fixed $t = 1$), and postulated a general scaling law

$$N(s) \propto s^{1-h} \qquad \text{for} \quad s \ll 1 \tag{1.6}$$

where $h - 1$ denotes the *index of self-similarity* of initial data (i.e., $h = 3/2$ for the Brownian motion and $h = 1/2$ for the white noise). The discussion of these and other types of Gaussian initial data can be found in an astrophysical paper by Vergassola *et al.*,[30] also for spatial dimension greater then 1.

The first rigorous result was Sinai's[25] theorem, which asserted that in the zero viscosity limit, the Hausdorff dimension of regular points for the Burgers stochastic flow with Brownian initial data is equal to 1/2 with probability 1. Avellaneda and E[2] proved a related result in the case of white-noise initial data. Namely, they demonstrated that

$$\mathbf{P}(s) \propto s^{1/2} \qquad \text{for} \quad s \ll 1 \tag{1.7}$$

where $\mathbf{P}(s)$ is the cumulative probability distribution of shock strengths.

In this paper we look at Sinai's problem in the context of heavy-tailed self-similar data of the Lévy α-stable type with the index of self-similarity equal to $1/\alpha$. We concentrate on the interval $1 < \alpha \leqslant 2$, where the Hausdorff dimension of regular points can be established, but also take a brief look at the asymmetric α-stable initial data with $0 < \alpha < 1$. In the absence of

analytic results, we rely on computer experimentation and statistical estimation techniques, as She *et al.*[24] did for the Gaussian case. Our experiments suggest that it is possible to extend Sinai's Theorem to α-stable motion initial data.

As an aside, let us just mention that the α-stable distributions are no strangers to astrophysical models. Apart from the Gaussian ($\alpha = 2$) and Cauchy ($\alpha = 1$) distributions, one of the first nontrivial stable distributions ($\alpha = 3/2$) was discovered in 1919 by Holtzmark,[10] who found it while studying random fluctuations of the gravitational field of stars in space considered as a "random aggregate" of points with "randomly varying masses."

The article is structured as follows. In Section 2 we briefly recall the method of construction of Lagrangian regular points in the Burgers equation, based on an application of the Legendre transform. Section 3 contains basic facts on approximation and computer simulation of the α-stable Lévy motion. These are quite nontrivial compared to the Gaussian case. The algorithm and the numerical strategy employed by us to construct the inverse Burgers Lagrangian function in the case of a trajectory of the α-stable Lévy motion as an initial condition are discussed in Section 4. In Section 5 we present qualitative aspects of the solutions together with heuristic interpretations. Section 6 is devoted to the statistical computer investigation of the Hausdorff dimension of regular points of solutions of the Burgers equation for several values of parameter α in the interval $1 < \alpha \leqslant 2$. Section 7 summarizes our main observations.

2. LEGENDRE TRANSFORM

In the inviscid limit, i.e., when $\nu \to 0$, the solutions to the Burgers equation (1.1) develop discontinuities (shocks) and can be interpreted as global solutions of the limiting Riemann equation only in the weak sense. In this situation, it is more convenient to deal with the limit of the velocity potential function $\psi = \psi(t, x; \nu)$ defined by (1.2). Taking $\nu \to 0$ in (1.2) and using the steepest descent argument, we get

$$\psi(t, x) = \max\{\psi_0(a) - (x-a)^2/(2t) : a \in \mathbb{R}\} \tag{2.1}$$

where $\psi_0 = \psi_0(a) = -\int_{-\infty}^{a} u_0(b)\, db$ is the initial potential.

Notice that with the use of the *Lagrangian potential*

$$\phi(t, a) \stackrel{\text{df}}{=} -\frac{a^2}{2} + t\psi_0(a) \tag{2.2}$$

and its *Legendre transform*

$$H_\phi(t, x) \stackrel{\text{df}}{=} \sup\{\phi(t, a) + xa : a \in \mathbb{R}\} \tag{2.3}$$

we can write formula (2.1) in the form

$$\psi(t, x) = \frac{H_\phi(t, x) - x^2/2}{t} \tag{2.4}$$

Making use of the crucial fact that

$$H_\phi \equiv H_{\bar{\phi}}$$

where $\bar{\phi} = \bar{\phi}(t, a)$ denotes the convex hull (envelope) of ϕ with respect to the space variable a, and defining the *Lagrangian map*

$$\mathscr{L}_t a \stackrel{\text{df}}{=} -\frac{\partial}{\partial a}\bar{\phi}(t, a) \tag{2.5}$$

we get the solution to the inviscid (i.e., zero viscosity limit) Burgers equation in the form

$$u(t, x) = u_0(\mathscr{L}_t^{-1} x)$$

where $\mathscr{L}_t^{-1}$ is the inverse of $\mathscr{L}_t$.

Let $a = a(t, x)$ denote any point where the maximum in (2.1) is attained. Function $a(t, x)$ as a function of the space variable x for a fixed time t is the principal object of study in this paper. In what follows $a = a(t, x)$ will be called the *inverse Lagrangian function* and $x = x(t, a)$—the (usual) *Lagrangian function*. Notice that

$$a(t, x') - a(t, x'') \geqslant 0 \qquad \text{for} \quad x' > x'' \tag{2.6}$$

which expresses the "sticky" property of shock fronts in Burgers turbulence; they may not pass through each other, while they may coalesce on collision. For some values of x, called *Eulerian shock points*, there exists a whole interval $[a^-, a^+]$, with $a^- = a(t, x-)$ and $a^+ = a(t, x^+)$, called the *Lagrangian shock interval*, where the maximum is achieved. For such values of x the Eulerian velocity $u(t, x)$ is discontinuous and has a jump (*shock amplitude*) of size

$$u^+ - u^- = -\frac{a^+ - a^-}{t} \tag{2.7}$$

which is proportional to the length of the Lagrangian shock interval. The union of all Lagrangian shock intervals $a \in [a^-, a^+]$ is called the set of *Lagrangian shock points.* The *set of Lagrangian regular points* is the complement of the union of the interiors (a^-, a^+) of all Lagrangian shock intervals.

It follows from the mass conservation principle that all particles, initially located in the interval $[a^-, a^+]$, have coalesced by the time t into the single Eulerian point x. In such a situation, we extend the Lagrangian map by imposing

$$\mathscr{L}_t a = x \qquad \text{for} \quad a \in [a^-, a^+] \tag{2.8}$$

In the numerical simulations presented below we construct directly the inverse Lagrangian map

$$\mathscr{L}_t^{-1} : x \to a(t, x) \tag{2.9}$$

by searching for the points maximizing (2.1) with fixed $t = 1$, getting $a(x) = \mathscr{L}_1^{-1} x$. The Eulerian velocity is then obtained as

$$u(t, x) = u_0(a(t, x)) = \frac{x - a(t, x)}{t} \tag{2.10}$$

All relations (2.1)–(2.10) are illustrated in Section 5 through a series of figures obtained on the basis of a fixed realization of initial data.

3. α-STABLE LEVY MOTION AND ITS SIMULATION

In this section we list some properties of α-stable random variables and introduce an α-stable Lévy motion, placed somewhere between Brownian motion and Poisson processes in the vast class of infinitely divisible processes, for which the structure of stochastic integrands and construction of the stochastic integrals are well understood (see, e.g., ref. 18). For further details concerning theoretical properties of α-stable random variables and processes see ref. 22. The numerical and statistical methods of their simulation are discussed in ref. 14.

The most common and convenient way to introduce α-stable random variables X is via their *characteristic functions* $\phi(\theta) = \mathbf{E} \exp(i\theta X)$, which depend on four parameters: α, the index of stability; β, the skewness

parameter; σ, the scale parameter; and μ, the shift. These functions are given by

$$\log \phi(\theta) = \begin{cases} -\sigma^{\alpha} |\theta|^{\alpha} \{1 - i\beta \operatorname{sgn}(\theta) \tan(\alpha\pi/2)\} + i\mu\theta, & \alpha \neq 1 \\ -\sigma |\theta| + i\mu\theta, & \alpha = 1 \end{cases} \tag{3.1}$$

where $\alpha \in (0, 2]$, $\beta \in [-1, 1]$, $\sigma \in \mathbb{R}_+$, $\mu \in \mathbb{R}$.

The fact that a random variable X has an α-stable distribution determined by (3.1) will be denoted $X \sim S_{\alpha}(\sigma, \beta, \mu)$. Note that $S_2(\sigma, 0, \mu)$ and $S_1(\sigma, 0, \mu)$ are, respectively, the Gaussian distribution $\mathcal{N}(\mu, 2\sigma^2)$ and the Cauchy distribution.

Working with α-stable distributions is complicated by the fact that, except for a few values of the parameters α, β, σ, and μ, explicit expressions for their density functions are not known. In computer simulations, an additional difficulty is that the convergence to a stable law in the corresponding central limit theorem is very slow, making the usual Gaussian random walk approach of little use. Our prior experience with computer experiments in this area[14] indicates that the best algorithm for generation of a quasirandom sample of X with a symmetric α-stable distribution $S_{\alpha}(1, 0, 0)$, $\alpha \in (0, 2]$, consists of the following two steps:

- Generate a random variable V uniformly distributed on $(-\pi/2, \pi/2)$ and an independent exponential random variable W with mean 1.
- Compute

$$X = \frac{\sin(\alpha V)}{\{\cos(V)\}^{1/\alpha}} \left\{ \frac{\cos(V - \alpha V)}{W} \right\}^{(1-\alpha)/\alpha} \tag{3.2}$$

The formula (3.2) can be extended to provide the following algorithm for simulation of a totally skewed stable random variable $X \sim S_{\alpha}(1, \beta, 0)$ with parameters $\alpha \in (0, 1)$ and $\beta = \pm 1$:

- Generate a random variable V uniformly distributed on $(-\pi/2, \pi/2)$ and an exponential random variable W with mean 1.
- Compute

$$X = D_{\alpha,\beta} \frac{\sin(\alpha(V + C_{\alpha,\beta}))}{\{\cos(V)\}^{1/\alpha}} \left\{ \frac{\cos(V - \alpha(V + C_{\alpha,\beta}))}{W} \right\}^{(1-\alpha)/\alpha} \tag{3.3}$$

where

$$C_{\alpha,\beta} = \frac{\arctan(\beta \tan(\pi\alpha/2))}{\alpha}, \qquad D_{\alpha,\beta} = \left[\cos\left(\arctan\left(\beta \tan\left(\frac{\pi\alpha}{2} \right) \right) \right) \right]^{-1/\alpha}$$

The proof that X defined by (3.3) has the $S_\alpha(1, \beta, 0)$-distribution can be obtained by a modification of the argument of Chambers *et al.*[5] Historically, the first computationally useful formula for simulation of α-stable random variables was suggested by Kanter[15] in the totally skewed case [formula (3.3)]. Then, on the basis of an integral formula from Ibragimov and Chernin,[13] Chambers *et al.* derived formula (3.2) and its generalizations. Formula (3.2) contains as a special case the well-known Box–Miller formula for generating normally distributed random variables.

Recall that α-stable Lévy motion $\{L_\alpha(t): t \geqslant 0\}$ is defined by the following properties:

(i) $L_\alpha(0) = 0$ a.s.

(ii) The process $\{L_\alpha(t): t \geqslant 0\}$ has independent increments.

(iii) $L_\alpha(t) - L_\alpha(s) \sim S_\alpha((t-s)^{1/\alpha}, \beta, 0)$ for any $0 \leqslant s < t < \infty$.

We are interested in investigating statistical solutions of the Burgers equation (1.1) with a trajectory of an α-stable Lévy motion (with $\alpha \in (1, 2]$) as initial data, i.e., we put

$$u_0(a) = \begin{cases} L_\alpha(a) & \text{for} \quad a \geqslant 0 \\ 0 & \text{for} \quad a < 0 \end{cases} \tag{3.4}$$

This initial condition assures self-similarity of solutions to the Burgers equation, since ($X \stackrel{\mathrm{d}}{=} Y$ means that X and Y have identical distributions)

$$L_\alpha(Ct) \stackrel{\mathrm{d}}{=} C^{1/\alpha} L_\alpha(t) \qquad \text{for} \quad C = \text{Const} > 0 \text{ and } t > 0 \tag{3.5}$$

which also assures the correctness of definition of ψ in (1.2). From (3.5), after integration, we get

$$\psi_0(Ca) \stackrel{\mathrm{d}}{=} C^{(\alpha+1)/\alpha} \psi_0(a)$$

and from (1.2) we derive

$$\psi(t, x) \stackrel{\mathrm{d}}{=} t^{(\alpha+1)/(\alpha-1)} \psi(1, xt^{\alpha/(\alpha-1)}) \tag{3.6}$$

and also

$$u(t, x) \stackrel{\mathrm{d}}{=} t^{1/(\alpha-1)} u(1, xt^{\alpha/(\alpha-1)}) \tag{3.7}$$

for $\alpha \in (1, 2]$.

The method of approximate computer simulation of an α-stable Lévy motion is based on the construction of a discrete-time process of the form

$$X_{t_i}^{\tau} = X_{t_{i-1}}^{\tau} + \Delta L_{\alpha,i}^{\tau}, \qquad i = 1,..., I \tag{3.8}$$

where $X_0^{\tau} = 0$ a.s. The set $\{t_i = i\tau : i = 0, 1,..., I\}$, $\tau = T/I$, provides a fixed-mesh partition of the interval $[0, T]$; the sequence of independent and identically distributed α-stable random variables $\Delta L_{\alpha,i}^{\tau}$ (playing the role of increments of $\{L_\alpha(t)\}$ over intervals $[t_{i-1}, t_i)$) is defined by

$$\Delta L_{\alpha,i}^{\tau} = L_\alpha(t_i) - L_\alpha(t_{i-1}) \sim S_\alpha(\tau^{1/\alpha}, \beta, 0) \sim \tau^{1/\alpha} S_\alpha(1, \beta, 0) \tag{3.9}$$

and, finally,

$$\Delta L_{\alpha,i}^{\tau} = \tau^{1/\alpha} X_i, \qquad i = 1, 2,..., I \tag{3.10}$$

where $\{X_i\}$ denotes a set of independent copies of X, constructed via (3.2) or (3.3).

It is not difficult to check that the finite-dimensional distributions of $\{X_{t_i}^{\tau}\}_{i=0}^{I}$ from (3.8), on subsets of the mesh $\{t_i\}_{i=0}^{I}$ are identical with the corresponding finite-dimensional distributions of the process $\{L_\alpha(t) : t \geqslant 0\}$. Furthermore, the above approximate method leads, in the limit when $\tau \to 0$, to the correct distribution on the space $\mathbb{D}([0, T], \mathbb{R})$ of right continuous sample paths with left limits.[16]

In order to adjust to the notation from the previous section, let us introduce a discrete function $\psi_0^{\tau} = \psi_0^{\tau}(a_i)$, which is obtained by numerical integration of the discretized initial condition $u_0^{\tau}(a_i) = X_{a_i}^{\tau}$, where $a_i = t_i = i \cdot \tau$. More precisely, $\psi_0^{\tau}(a_i) = 0$ for $i = 0, -1, -2,...$, and

$$\psi_0^{\tau}(a_i) = -\tau \left(\sum_{l=1}^{i-1} X_{a_l}^{\tau} + \tfrac{1}{2} X_{a_i}^{\tau} \right) \qquad \text{for} \quad i = 1, 2,... \tag{3.11}$$

Formula (3.11) is a discrete (obtained via the "trapezoid method" of numerical integration) counterpart of the relation $\psi_0(a) = -\int_{-\infty}^{a} u_0(b)\, db$.

4. NUMERICAL ALGORITHMS AND COMPUTER SIMULATIONS

Due to self-similarity [properties (3.5) and (3.7)] of the initial data ψ_0^{τ} and of the solution $u = u(t, x)$, we can restrict our attention to the solution at fixed time, say $t = 1$, and construct and study only functions

$$a = a(x) \overset{\text{df}}{=} a(1, x), \qquad x = x(a) \overset{\text{df}}{=} x(1, a)$$

where $a(t, x), x(t, a)$ are defined by (2.1) and (2.8). So, for a particle initially (at time $t=0$) at position a, $x(a)$ denotes its position at time $t=1$. Conversely, if $a=a(x)$ is continuous at x, $a(x)$ denotes the initial position of a particle which at time $t=1$ is located at x. If $a=a(x)$ is discontinuous at x, then the interval $[a(x-), a(x+)]$ describes initial positions of points a which form a "cluster" at x at time $t=1$. This is illustrated in Fig. 7. The method based on construction of convex envelopes for given Lagrangian potential functions $\phi=\phi(a)=\phi(1, a)$ also leads to the same structure of shock fronts, even when ϕ is not differentiable [i.e., when the initial velocity field (3.4), approximated by (3.10), is discontinuous]. This is shown on Fig. 8.

With the initial data defined by (3.11), we obtain a discrete analogue of (2.1), which can be rewritten in the following way

$$\psi^{\tau,\kappa}(x_j)=\max\{\psi_0^{\tau}(a_i)-(x_j-a_i)^2/2: i\in\{\ldots,-2,-1,0,1,2,\ldots,I,\ldots\}\} \quad (4.1)$$

where $\{x_j\}_{j=0}^{J}$ denotes a discrete set of values of x, defined as $x_j=x_{\min}+\kappa\cdot j$, for $j=0, 1,\ldots, J$, $\kappa=^{\mathrm{df}}(x_{\max}-x_{\min})/J$, with fixed values of $x_{\min}$, $x_{\max}$. For a fixed x_j, the value of a_i for which the maximum in (4.1) is attained will be denoted by $a^{\tau,\kappa}(x_j)$, i.e., $a(x_j)\approx a^{\tau,\kappa}(x_j)$.

Starting with explicitly computed values of $\psi^{\tau,\kappa}(x_j)$ corresponding to the set of nonpositive a_i, we can proceed recursively with respect to the range of values of a_i in (4.1). Having at our disposal sets of values $\{\psi^{\tau,\kappa}(x_j)\}_{j=0}^{J}$ and $\{a^{\tau,\kappa}(x_j)\}_{j=0}^{J}$ determined for $\{a_i: i\leqslant I\}$, it is sufficient to add the next point a_{I+1} to the right-hand side of (4.1) and, making use of monotonicity of the inverse Lagrangian function $a=a(x)$, to check which values of $\psi^{\tau,\kappa}(x_j)$ and $a^{\tau,\kappa}(x_j)$ increase. More details on different aspects of such computer algorithms can be found in ref. 24, where a similar approach is described. In our approach we pay more attention to certain statistical features of the algorithm involving the Lagrangian potential. Instead of looking at a fixed realization (trajectory) of the Lagrangian potential, we control some statistical properties of a stochastic process

$$\Phi(a)=\Phi(a,\omega)\stackrel{\mathrm{df}}{=}\phi(a)=\phi(a,\omega), \qquad a\geqslant 0 \quad (4.2)$$

where $\phi(a,\omega)=\phi(a)$ denotes the Lagrangian potential function corresponding to a single realization of an α-stable Lévy motion process [for a fixed $\omega\in\Omega$ in the underlying probability space $(\Omega, \mathcal{F}, P)$]. Using numerical, statistical, and computer techniques described in detail in ref. 14, it is possible to construct this process for any α-stable initial data (3.4). The results presented on Fig. 9 suggest a kind of stochastically continuous and

monotonic dependence of the process Φ on α. At the same time, they explain why it is possible to get appropriate statistical samples of shock fronts for "practically all" corresponding trajectories of an α-stable Lévymotion process, and to construct acceptable estimators of their cumulative probability functions.

The problem of estimation of errors $a(x_j) - a^{\tau,\kappa}(x_j)$ and of their impact on the correctness of calculated approximate values of the Hausdorff dimension of sets of Lagrangian regular points (which exhibit a fractal structure) is quite nontrivial and it would be worthwhile to investigate it more thoroughly in the future. However, a careful design of our computational experiments allows us to select appropriate values of τ and κ which satisfy some obvious stability requirements. In particular, our results display a convergent behavior as values of τ and κ decrease, thus assuring sensitive detection of discontinuities (upward jumps) of $a(x)$, and exhibit a discrete analogue of the self-similarity in computed and "zoomed-in" discrete data. Also, an experiment consisting of computation of shock intervals $[a^-, a^+]$ by two different methods–one based on relation (4.1) and the other utilizing a construction of the convex envelope for the Lagrangian potential–confirms the correctness of the numerical results (see Fig. 8).

Our practical strategy, slightly different from that suggested by She *et al.*,[24] and implemented on a relatively simple 85-MHz Pentium processor, was to produce a set of data for which the constructed fractal-like sets of Lagrangian regular points display a behavior reflecting the behavior conjectured in this paper, and rigorously proven by Sinai[25] for the Brownian initial data. This is achieved by repeated simulations of independent realizations of the process $\Phi = \Phi(a)$ and of corresponding inverse Lagrangian functions $a = a(x)$ providing statistical samples of shock intervals containing, on the average, about 100,000 trials. The results derived from computer simulations are close to the conjectured ones. In addition, monotonicity of the estimated Hausdorff dimension of regular Lagrangian points as a function of the parameter α varying from $\alpha = 2$ to $\alpha = 1$ provides a supplementary argument for their validity.

One final remark is in order. The sample paths of the α-stable Lévy motion are discontinuous. With a discontinuous initial velocity the corresponding convex hull may have corner points and its derivative can be discontinuous. Therefore, for an individual sample path, some part of space can be void of any mass and numerical results concern only the points where the derivative is continuous. This, however, ceases to be a problem with repeated sampling of the trajectories since the α-stable Lévy motion is stochastically continuous and has no fixed discontinuities where a positive jump would occur at a fixed point with positive probability.

5. QUALITATIVE FEATURES OF THE SOLUTIONS

Having obtained sets of values $\{a^{\tau,\kappa}(x_j)\}_{j=0}^{J}$, we can analyze their fractal structure, verifying whether they display the power-law behavior similar to that in (1.5) or (1.7).

To get a first insight into the properties of statistical solutions of the initial value problem (1.1) with α-stable data, we present a series of figures containing graphs of the Lagrangian inverse function $a = a(x)$ obtained from computer simulations for two different values of parameter α, $\alpha = 2.0$ and $\alpha = 1.5$. Similar to the Brownian motion case $\alpha = 2$, the graphs show *devil's staircases* for $\alpha \in (1, 2)$ as well, the effect confirmed by zooming in on details as shown in Figs. 1–4. A closer look at our results indicates that, for the α-stable Lévy motion as initial velocity, the total number of shocks per unit length is infinite and that the Euler shock points are dense. The latter effect becomes more pronounced when α approaches 1, which is somewhat surprising and seems to contradict naive guesses. However, it can be explained by the fact that typical trajectories of the α-stable Lévy motions display, as $\alpha \searrow 1$, an increasing number of very small jumps.

For comparison, we have also considered another family of self-similar α-stable initial data belonging to the class of *subordinated* Lévy α-stable processes, namely the Lévy stable motion with $\alpha \in (0, 1)$ and $\beta = -1$. Its increments have *totally skewed* distributions $S_\alpha(1, -1, 0)$, so only jumps in one direction are possible. Figure 5 and 6 present typical results of simulation for this range of parameters. In this case, despite the self-similar initial data, the set of regular points of the Lagrangian map displays no obvious fractal behavior.

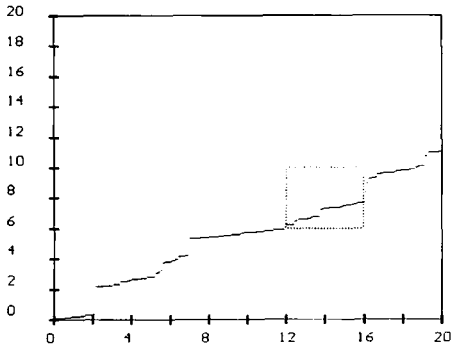

Fig. 1. Inverse Lagrangian function $a = a(x)$ corresponding to the solution of the inviscid Burgers equation at $t = 1$, with a trajectory of the α-stable Lévy motion ($\alpha = 2.0$) as the initial velocity (a versus x plot).

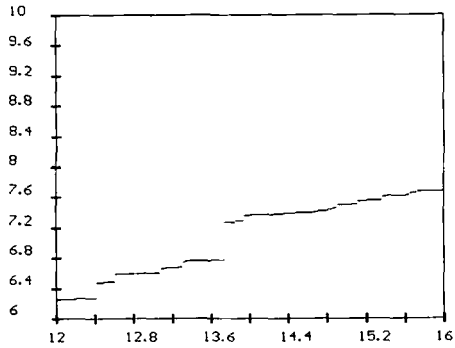

Fig. 2. Zoomingin on finer structures of the above graph of Fig. 1.

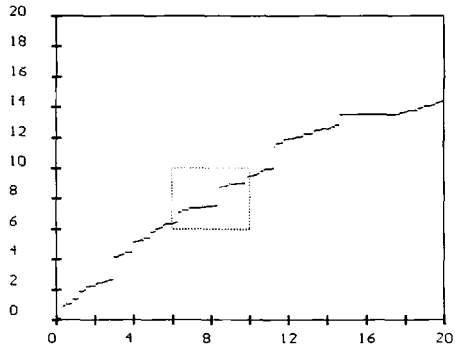

Fig. 3. Inverse Lagrangian function $a = a(x)$ corresponding to the solution of the inviscid Burgers equation at $t = 1$, with a trajectory of the α-stable Lévy motion ($\alpha = 1.5$) as the initial velocity (a versus x plot).

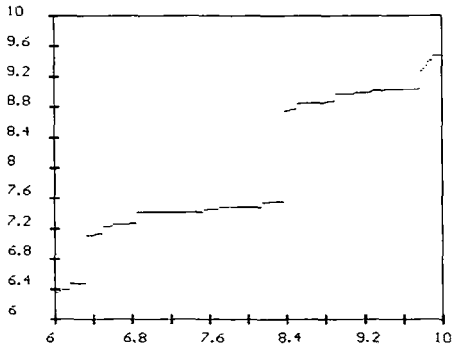

Fig. 4. Zoomingin on finer structures of the graph of Fig. 3.

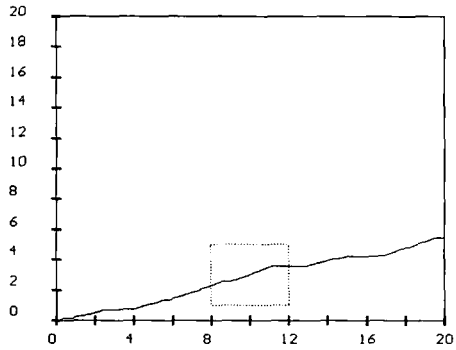

Fig. 5. Inverse Lagrangian function $a = a(x)$ corresponding to the solution of the inviscid Burgers equation at $t = 1$, with a trajectory of the *totally skewed* α-stable Lévy motion ($\alpha = 0.75$, $\beta = -1$) as the initial velocity (a versus x plot).

Figures 7 and 8 are intended to illustrate the "Eulerian–Lagrangian machinery" presented in Section 2 and utilized in our study of statistical properties of solutions to the Burgers equation.

Let us emphasize that all four graphs presented in Figs. 7 and 8 describe the results of a computer experiment with the same fixed realization of the potential $\psi_0 = \psi_0(a)$ given by (3.11).

It is impossible to make any comparison of results obtained for different values of α on the basis of one realization of the α-stable Lévy motion (as presented in Figs. 1–4), because of an enormous spread of possible results. Thus one has to consider statistical features of the Lagrangian map $\phi = \phi(a)$ considered as a stochastic process. These are

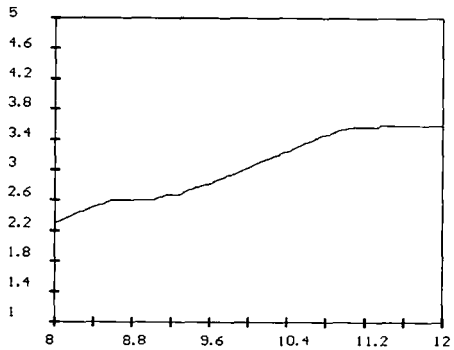

Fig. 6. Zoomingin on finer structures of the graph of Fig. 5.

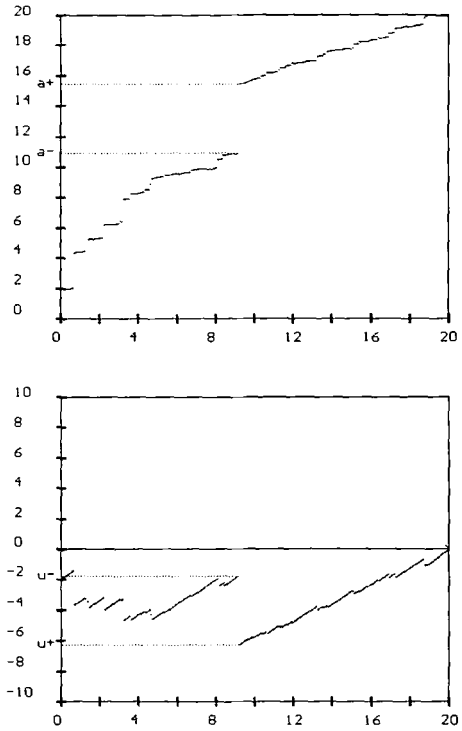

Fig. 7. Plots of the inverse Lagrangian function $\mathscr{L}_1^{-1}x = a(x)$ and the corresponding solution $u = u(x)$ as functions of x. Function u solves the inviscid Burgers equation at $t = 1$, with a trajectory of the α-stable Lévy motion ($\alpha = 1.75$) as the initial velocity (the largest jump of a and u, corresponding to the same value of x, is indicated).

presented on Fig. 9 in the form of deciles, revealing a continuous dependence of this process on parameter α.

6. FRACTAL STRUCTURE OF LAGRANGIAN REGULAR POINTS

Surveying various practically useful methods of studying the fractal structure of experimental data (see, e.g; ref. 6), we found that the method based on the calculation of the cumulative frequency distributions of gaps between consecutive jumps of $a = a(x)$ was best suited to our purposes. Given our emphasis on working with minimal sets of data that would give significant results, our choice was also influenced by the example of a study

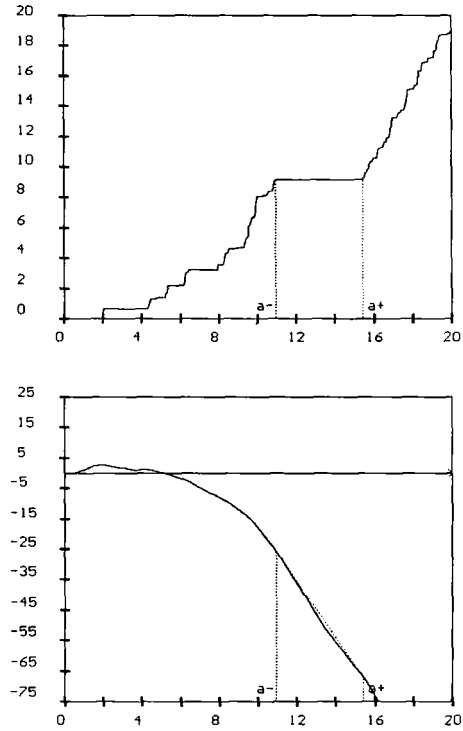

Fig. 8. Plots of the Lagrangian map $\mathscr{S}_1 a = x(a)$ and the Lagrangian potential $\phi = \phi(a)$ as functions of a. They correspond to the solution of the inviscid Burgers equation at $t = 1$, with a trajectory of the α-stable Lévy motion ($\alpha = 1.75$) as the initial velocity (only the largest shock interval is indicated).

of the fractal structure of Japanese earthquake data,[29] where a comparatively small data set was available. The method consists in:

- Simulation of realizations of initial data $\{\psi_0^{\tau}(a_i): i = 0, 1, \ldots\}$.
- Computation of values of the corresponding function $\{a^{\tau,\kappa}(x_j)\}_{j=0}^{J}$.
- Calculation of statistical frequencies of gaps (x^-, x^+) between consecutive points x^- and x^+ of discontinuity of $a = a(x)$.
- Estimation of a value of the scaling parameter H under the assumption that the corresponding set of regular Lagrangian points described by intervals (x^-, x^+) exhibits the power-law behavior with scaling parameter H.

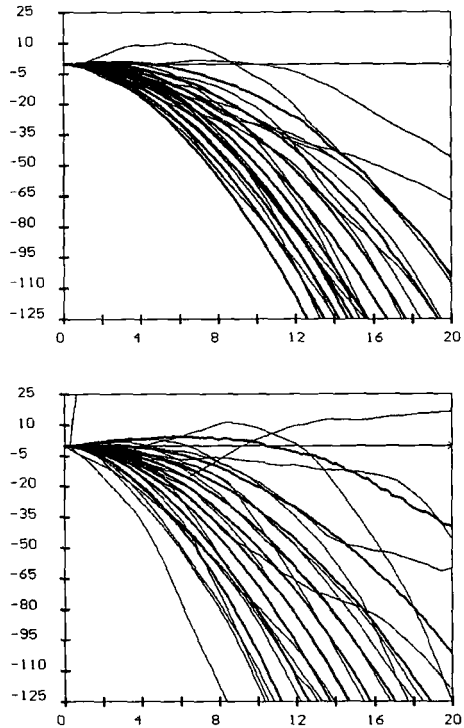

Fig. 9. Plots of the Lagrangian potential Φ defined by (4.2) versus a, for $\alpha = 2.0$ (top) and $\alpha = 1.5$ (bottom). This stochastic process is visualized here through a display of 20 realizations (thin lines) and 9 quantile (decile) lines $q_{p_i} = q_{p_i}(a)$ (thick lines), defined by the relation $P\{\phi(a) > q_{p_i}(a)\} = p_i$, for $p_i \in \{0.1, 0.2, \ldots, 0.9\}$, and estimated on the basis of 5000 independent approximate trajectories of Φ.

So the final step of the algorithm consists in estimating the value of H such that

$$\#\{(x^-, x^+): x^+ - x^- > \Delta x\} \approx \text{Const} \cdot (\Delta x)^{-H} \tag{6.1}$$

It follows from Mandelbrot's theorem[19] that the above algorithm producing (approximately) the cumulative frequency distribution of Lagrangian shock intervals $[a^-, a^+]$, provides the Hausdorff dimension H of the corresponding fractal set of Lagrangian regular points in $\mathbb{R}$.

Figures 10–13 show the results of numerical computations of approximate values of the Hausdorff dimension H for the set of values of $\{a^{\tau,\kappa}(x_j)\}_{j=0}^{J}$ derived from (4.1). Values of the parameter $\alpha = 2.0$, 1.75, 1.5,

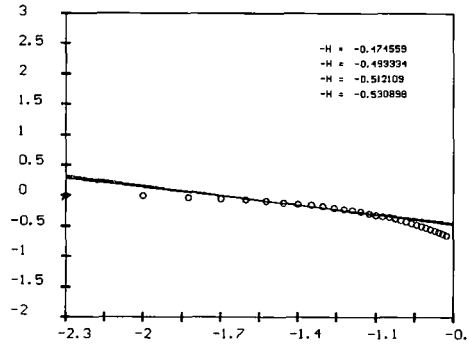

Fig. 10. The tail cumulative frequency distribution of intervals between jumps of the inverse Lagrangian function $a = a(x)$ corresponding to the solution of the inviscid Burgers equation at $t = 1$, with the symmetric α-stable Lévy motion trajectory ($\alpha = 2.0$) as the initial velocity; presented as a log–log plot.

and 1.25 were considered for the same values of all other parameters included in the computer algorithm (e.g., $\tau = 0.001$, $\kappa = 0.0025$, $I = 100{,}000$) were used. Notice that (6.1) can be rewritten in the form

$$\log \mathbf{P}\{x^+ - x^- > \Delta x\} \approx -H \log(\Delta x) + D \tag{6.2}$$

so the results are plotted on log–log scales. The horizontal axis is the logarithm of the size of gaps, and the vertical axis is the logarithm of the tail cumulative statistical frequency (calculated on the basis of approximately $100 \times 5{,}000$ realizations[3]) of sizes of gaps (x^-, x^+) between consecutive points x^- and x^+. Each circle represents data for one of the 30 selected values of Δx.

Before doing the linear least-squares fit, the data points for small and large values of Δx had to be removed. The data corresponding to small values of Δx, which represent frequencies of small-size shocks, are not reliable because the grid size limits the ability to accurately decide if small jumps actually occur. On the other hand, in view of the theoretical results (see ref. 2 for the case $\alpha = 2$), we know that the large shocks follow a different law.

The selection of lower and upper cutoff points was done using the case $\alpha = 2$ and Sinai's theoretical result for calibration purposes. Thus data points number 1, 2, and 3 (counting from the left) were dropped. The upper cutoff points were selected to be the data points number 12, 13, 14,

[3] One hundred repeated computations of $a = a(x)$ involving 5000 approximate values $a^{\tau,\kappa}(x_j)$.

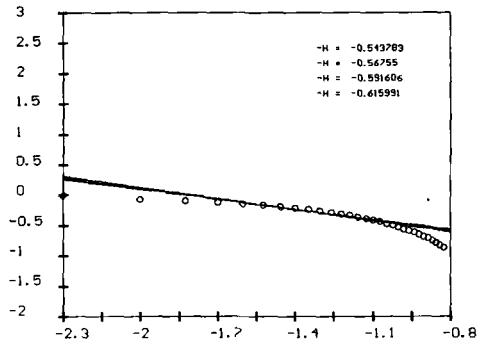

Fig. 11. The tail cumulative frequency distribution of intervals between jumps of the inverse Lagrangian function $a = a(x)$ corresponding to the solution of the inviscid Burgers equation at $t = 1$, with the symmetric α-stable Lévy motion trajectory ($\alpha = 1.75$) as the initial velocity, presented as a log–log plot.

and 15, which gave us four regression lines shown on each of Figs. 10–13. Their slopes bracket the estimated Hausdorff dimension H. Note that in ref. 24 the fitting for the case $\alpha = 2$ was displayed for a narrower set of data corresponding roughly to the interval $(-1.7, -1)$ on our Fig. 7. We decided to display the entire picture as it illuminates the whole situation well and is typical whenever one tries to numerically compute the power-law behavior (see, e.g., ref. 6).

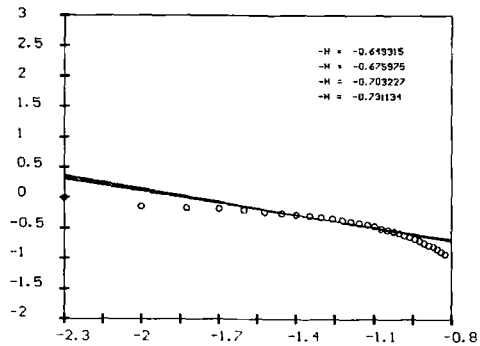

Fig. 12. The tail cumulative frequency distribution of intervals between jumps of the inverse Lagrangian function $a = a(x)$ corresponding to the solution of the inviscid Burgers equation at $t = 1$, with the symmetric α-stable Lévy motion trajectory ($\alpha = 1.5$) as the initial velocity, presented as a log–log plot.

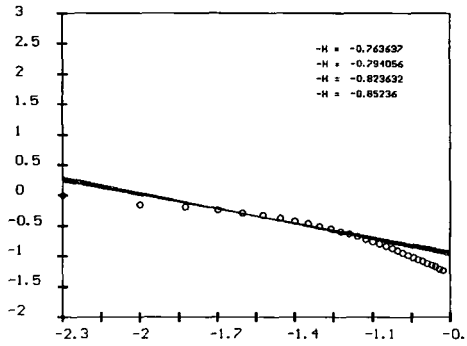

Fig. 13. The tail cumulative frequency distribution of intervals between jumps of the inverse Lagrangian function $a = a(x)$ corresponding to the solution of the inviscid Burgers equation at $t = 1$, with the symmetric α-stable Lévy motion trajectory ($\alpha = 1.25$) as the initial velocity, presented as a log–log plot.

Note that the inclusion of data points 4–13 and 4–14 results in bracketing:

$$H = 1/2 + \begin{cases} +0.007 \\ -0.007 \end{cases} \quad \text{for} \quad \alpha = 2.00$$

$$H = 4/7 + \begin{cases} +0.004 \\ -0.020 \end{cases} \quad \text{for} \quad \alpha = 1.75$$

$$H = 2/3 + \begin{cases} +0.009 \\ -0.033 \end{cases} \quad \text{for} \quad \alpha = 1.50$$

$$H = 4/5 + \begin{cases} +0.006 \\ -0.024 \end{cases} \quad \text{for} \quad \alpha = 1.25$$

7. CONCLUSIONS

The present computer study of statistical properties of shocks in the solutions of the inviscid Burgers equation with the initial data of α-stable type strongly indicates that the scaling properties of the data carry over to the fractal structure of regular points of the Lagrangian maps if $1 < \alpha \leqslant 2$. In particular it suggests the following:

Conjecture. Let $1 < \alpha \leqslant 2$. The set of Lagrangian regular points of the statistical solution (1.2) of the Burgers equation (1.1) with the α-stable Lévy motion as initial data has Hausdorff dimension $1/\alpha$.

For completely asymetric α-stable initial data with $0 < \alpha < 1$, the simulations indicate that the conjecture is no longer true.

The rigorous proof of the above conjecture cannot simply follow the lines of Sinai's proof for the case $\alpha = 2$, which very strongly depends on specific properties of the convex envelope of the Lagrangian potential with Brownian initial data. The situation is much more complex in the α-stable case, although then, in a sense, the law of the iterated logarithm has a simpler form.

ACKNOWLEDGMENTS

This research was partly supported by grants from the Office of Naval Research and the National Science Foundation. The authors would also like to thank anonymous referees for their help in improving the original version of this paper.

REFERENCES

1. S. Albeverio, S. A. Molchanov, and D. Surgailis, Stratified structure of the Universe and Burgers' equation: A probabilistic approach, *Prob. Theory Rel. Fields* **100**:457–484 (1994).
2. M. Avellaneda and W. E, Statistical properties of shocks in Burgers turbulence, *Commun. Math. Phys.* **172**:13–38 (1995).
3. A. V. Bulinskii and S. A. Molchanov, Asymptotic Gaussianness of solutions of the Burgers equation with random initial data, *Teorya Veroyat. Prim.* **36**:217–235 (1991).
4. J. M. Burgers, *The Nonlinear Diffusion Equation* (Reidel, Dordrecht, 1974).
5. J. M. Chambers, C. L. Mallows, and B. Stuck, A method for simulating stable random variables, *J. Am. Stat. Assoc.* **71**:340–344 (1976).
6. C. D. Cutler, Some results on the behavior and estimation of the fractal dimensions of distributions on attractors, *J. Stat. Phys.* **62**:651–708 (1991).
7. T. Funaki, D. Surgailis, and W. A. Woyczynski, Gibbs–Cox random fields and Burgers turbulence, *Ann. Appl. Prob.* **5**:701–735 (1995).
8. T. Gotoh and R. H. Kreichnan, Statistics of decaying Burgers turbulence, *Phys. Fluids A* **5**:445–457 (1993).
9. S. N. Gurbatov, A. N. Malakhov, and A. I. Saichev, *Nonlinear Random Waves in Dispersionless Media* (Nauka, Moscow, 1990).
10. J. Holtzmark, Über die Verbreiterung von Spektrallinien, *Ann. Phys. (Leipzig)* **58**:577–630 (1919).
11. Y. Hu and W. A. Woyczynski, An extremal rearrangement property of statistical solutions of the Burgers equation, *Ann. Appl. Prob.* **4**:838–858 (1994).
12. Y. Hu and W. A. Woyczynski, Shock density in Burgers' turbulence, in *Nonlinear Stochastic PDE's: Burgers Turbulence and Hydrodynamic Limit* (Springer-Verlag, Berlin, 1995), pp. 201–213.
13. I. A. Ibragimov and K. E. Chernin, On the unimodality of stable laws, *Theory Prob. Appl.* **4**:453–456 (1959).
14. A. Janicki and A. Weron, *Simulation and Chaotic Behavior of α-Stable Stochastic Processes* (Marcel Dekker, New York; 1994).

15. M. Kanter, Stable densities under change of scale and total variation inequalities, *Ann. Prob.* **3**:697–707 (1975).
16. Y. Kasahara and K. Yamada, Stability theorem for stochastic differential equations with jumps, *Stoch. Proc. Appl.* **38**:13–32 (1991).
17. S. Kida, Asymptotic properties of Burgers turbulence, *J. Fluid Mech.* **79**:337–377 (1977).
18. S. Kwapien and W. A. Woyczynski, *Random Series and Stochastic Integrals; Single and Multiple* (Birkhäuser; Boston, 1992).
19. B. Mandelbrot, *The Fractal Geometry of Nature* (Freeman, San Francisco, 1982).
20. S. A. Molchanov, D. Surgailis, and W. A. Woyczynski, Hyperbolic asymptotics in Burgers' turbulence and extremal processes, *Commun. Math. Phys.* **165**:209–226 (1995).
21. M. Rosenblatt, Scale renormalization and random solutions of the Burgers equation, *J. Appl. Prob.* **24**:328–338 (1987).
22. G. Samorodnitsky and M. S. Taqqu, *Stable non-Gaussian Random Processes: Stochastic Models with Infinite Variance* (Chapman and Hall, London, 1994).
23. S. F. Shandarin and Ya. B. Zeldovich, Turbulence, intermittency, structures in a self-gravitating medium: The large scale structure of the Universe, *Rev. Mod. Phys.* **61**:185–220 (1989).
24. Z.-S. She, E. Aurell, and U. Frisch, The inviscid Burgers equation with initial data of Brownian type, *Commun. Math. Phys.* **148**:623–641 (1992).
25. Ya. G. Sinai, Statistics of shocks in solutions of inviscid Burgers equation, *Commun. Math. Phys.* **148**:601–621 (1992).
26. D. Surgailis and W. A. Woyczynski, Long range prediction and scaling limit for statistical solutions of the Burgers' equation, in *Nonlinear Waves and Weak Turbulence* (Birkhäuser, Boston, 1993), pp. 313–338.
27. D. Surgailis and W. A. Woyczynski, Burgers' equation with nonlocal shot noise data, *J. Appl. Prob.* **31A**:351–362 (1994).
28. D. Surgailis and W. A. Woyczynski, Scaling limits of solutions of Burgers' equation with singular Gaussian initial data, in *Chaos Expansions, Multiple Wiener–Itô Integrals and Their Applications*, C. Houdré and V. Perez-Abreu, eds. (CRC Press, Boca Raton, Florida, 1994), pp. 145–162.
29. T. Utsu, A catalog of large earthquakes in Japan for the years 1885–1925, in *Historical Seismographs of Earthquakes of the World*, W. H. K. Lee, H. Meyers, and K. Shimazaki, eds. (Academic Press, San Diego, California, 1988), pp. 150–161.
30. M. Vergassola, B. Dubrulle, U. Frisch, and A. Noullez, Burgers' equation, devil's staircases and the mass distribution for large-scale structures, *Astron. Astrophys.* **289**:325–356 (1994).
31. W. A. Woyczynski, Stochastic Burgers' flows, in *Nonlinear Waves and Weak Turbulences* (Birkhäuser, Boston, 1993), pp. 279–311.